

See discussions, stats, and author profiles for this publication at: <https://www.researchgate.net/publication/224139290>

# Magnetic Navigation System With Gradient and Uniform Saddle Coils for the Wireless Manipulation of Micro-Robots in Human Blood Vessels

Article in IEEE Transactions on Magnetics · July 2010

DOI: 10.1109/TMAG.2010.2040144 · Source: IEEE Xplore

CITATIONS

58

READS

768

4 authors:



**Seungmun Jeon**

Kongju National University

14 PUBLICATIONS 145 CITATIONS

[SEE PROFILE](#)



**Gunhee Jang**

Indiana University Bloomington

176 PUBLICATIONS 1,673 CITATIONS

[SEE PROFILE](#)



**Hyunchul Choi**

Chonnam National University

46 PUBLICATIONS 366 CITATIONS

[SEE PROFILE](#)



**Sukho Park**

Daegu Gyeongbuk Institute of Science and Technology

623 PUBLICATIONS 8,900 CITATIONS

[SEE PROFILE](#)

# Magnetic Navigation System With Gradient and Uniform Saddle Coils for the Wireless Manipulation of Micro-Robots in Human Blood Vessels

Seungmun Jeon<sup>1</sup>, Gunhee Jang<sup>1</sup>, Hyunchul Choi<sup>2</sup>, and Sukho Park<sup>2</sup>

<sup>1</sup>PREM, Department of Mechanical Engineering, Hanyang University, Seoul 133-791, Korea

<sup>2</sup>Department of Mechanical Engineering, Chonnam National University, Gwangju 500-757, Korea

A magnetic navigation system (MNS) for the wireless manipulation of micro-robots in human blood vessels is a possible surgical tool for coronary artery disease. This paper proposes a novel MNS composed of one conventional pair of Maxwell and Helmholtz coils and one newly developed pair of gradient and uniform saddle coils. The proposed system was theoretically developed using the Biot-Savart law, and it was verified experimentally after constructing the proposed MNS. The proposed MNS is geometrically compact to allow a patient to lie down, and magnetically efficient compared with the conventional MNS which has two pairs of Maxwell and Helmholtz coils.

**Index Terms**—Gradient saddle coil, magnetic navigation system, micro-robot, uniform saddle coil.

## I. INTRODUCTION

CORONARY artery diseases such as angina pectoris and myocardial infarction have been the major causes of human death in modern society [1]. One of the treatments is a surgical operation known as percutaneous coronary intervention which uses a catheter inserted and controlled by a medical doctor to unclog a clogged blood vessel or to enlarge a narrow blood vessel [2]. In some cases, catheters are difficult to control, and may suffer from size limitation. Several researchers have investigated the use of wireless micro-robots driven by magnetic navigation system (MNS) as an alternative to percutaneous coronary intervention [3]–[6]. Since the manipulating power of the micro-robot is dependent on the magnetic field generated by the MNS, the micro-robot does not require additional batteries, and the complexity and size of the micro-robot can be reduced to effectively navigate through twisted narrow blood vessels.

Several researchers have shown that a micro-robot can be manipulated by a conventional MNS consisting of Helmholtz and Maxwell coils [5], [6]. Yesin *et al.* experimentally demonstrated that a MNS with one pair of Helmholtz and Maxwell coils can generate the plane motion of a micro-robot by mechanically rotating the MNS [5]. Choi *et al.* showed that a MNS with two stationary pairs of Maxwell and Helmholtz coils can manipulate a micro-robot in a plane [6]. However, this system suffers from the geometrical weakness such that the radius of one pair should be at least twice as large as that of the other pair. This increases the amount of space required by the MNS, and requires a great amount of electrical power to generate an effective magnetic field.

This research proposes a novel MNS shown in Fig. 1, composed of one conventional pair of Maxwell and Helmholtz coils

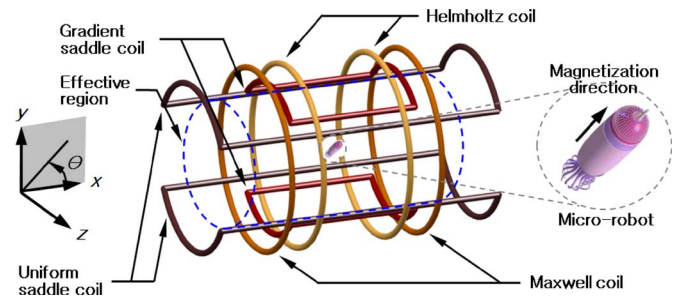


Fig. 1. Proposed novel magnetic navigation system.

and one newly developed pair of gradient and uniform saddle coils. It determines the relationships of the currents in each coil to generate the magnetic force and torque. It also compares the magnetic force and torque generated by the proposed MNS to those of the conventional MNS and demonstrates the effectiveness of the proposed MNS. This research then verifies the efficacy of the proposed MNS by carrying out experiments exploring plane motions of a micro-robot.

## II. THEORETICAL DEVELOPMENT OF THE NOVEL MNS

Magnetic forces and torques applied to a micro-robot composed of permanent magnetic material in a magnetic field can be expressed by the following equations:

$$\vec{F} = \mu_0 V (\vec{M} \cdot \nabla) \vec{H} \quad (1)$$

$$\vec{T} = \mu_0 V \vec{M} \times \vec{H} \quad (2)$$

where  $\mu_0$ ,  $V$ ,  $\vec{M}$ , and  $\vec{H}$  are the magnetic permeability of free space, the volume, the magnetization of a micro-robot, and the magnetic field intensity, respectively. The magnetic force is proportional to the magnetic field gradient and the magnetic torque is proportional to the magnetic field intensity.

### A. Conventional Maxwell and Helmholtz Coils

A Maxwell coil is composed of two identical coils separated by the distance of  $\sqrt{3}$  times the coil radius. The currents in the

Manuscript received October 31, 2009; accepted January 02, 2010. Current version published May 19, 2010. Corresponding author: G. H. Jang (e-mail: ghjang@hanyang.ac.kr).

Color versions of one or more of the figures in this paper are available online at <http://ieeexplore.ieee.org>.

Digital Object Identifier 10.1109/TMAG.2010.2040144

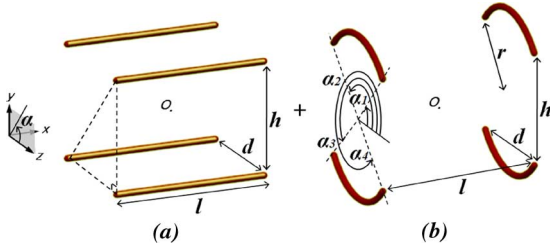


Fig. 2. Geometries of (a) straight and (b) arc coils.

coils flow in opposite directions. The magnetic field induced from a current source can be determined by the Biot-Savart's law, and the magnetic field near the center of the Maxwell coil shown in Fig. 1 can be expressed as follows [6]:

$$\vec{H}_m = [g_m x - 0.5g_m y - 0.5g_m z]^T \quad (3)$$

$$g_m = \frac{16}{3} \left( \frac{3}{7} \right)^{\frac{5}{2}} \frac{i_m}{r_m^2} \quad (4)$$

where  $i_m$  and  $r_m$  are the current and radius of the Maxwell coil, respectively. Equation (3) shows that the Maxwell coil generates the largest uniform magnetic field gradient along the  $x$ -axis. From (1), the Maxwell coil can generate uniform magnetic force to propel a micro-robot if a micro-robot is located near the center of the coil and if the magnetization direction of the micro-robot is aligned along the  $x$ -axis.

The magnetic field near the center of the Helmholtz coil in Fig. 1 can be expressed as follows [6]:

$$\vec{H}_h = [d_h \ 0 \ 0]^T \quad (5)$$

$$d_h = \left( \frac{4}{5} \right)^{\frac{3}{2}} \frac{i_h}{r_h} \quad (6)$$

where  $i_h$  and  $r_h$  are the current and radius of the Helmholtz coil, respectively. Since the Helmholtz coil generates a uniform magnetic field intensity along the  $x$ -axis, the Helmholtz coil can generate uniform magnetic torque to align a micro-robot located near the center of the coil along the  $x$ -axis.

### B. Proposed Gradient and Uniform Saddle Coils

This research develops saddle-shaped coils referred to as gradient and uniform saddle coils as shown in Fig. 1. Since each coil is intended to replace the  $y$ -directional Maxwell and Helmholtz coils of the conventional MNS in [6], they should generate a uniform magnetic field gradient and intensity along the  $y$ -direction, respectively. They are composed of the straight and arc coils as shown in Fig. 2(a) and (b), and the magnetic fields can be determined by the summation of each straight and arc coils. The magnetic fields of general straight and arc coils along the  $y$ -axis in Fig. 2 can be expressed as follows:

$$H_y^{st} = \frac{ad^2 i}{4\pi} \left( \left( \frac{d^2}{4} + \left( \frac{h}{2} - y \right)^2 \right)^{-1} \times \left( \frac{d^2}{4} (1 + a^2) + \left( \frac{h}{2} - y \right)^2 \right)^{-\frac{1}{2}} \right)$$

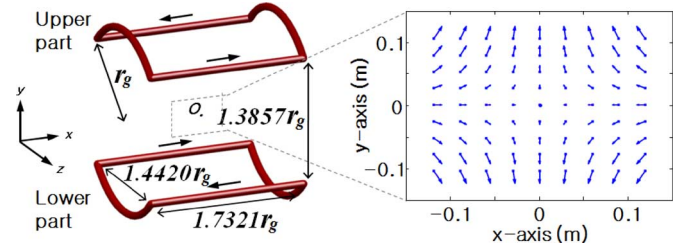


Fig. 3. Geometrical relationship and magnetic field of the gradient saddle coil.

$$\mp \left( \frac{d^2}{4} + \left( \frac{h}{2} + y \right)^2 \right)^{-1} \times \left( \frac{d^2}{4} (1 + a^2) + \left( \frac{h}{2} + y \right)^2 \right)^{-\frac{1}{2}} \quad (7)$$

$$H_y^{arc} = \frac{adri}{4\pi} \left( \int_{\alpha_1}^{\alpha_2} \sin \alpha \left( \left( \frac{ad}{2} \right)^2 + (r \cos \alpha)^2 + (y - r \sin \alpha)^2 \right)^{-\frac{3}{2}} d\alpha \right. \\ \left. \pm \int_{\alpha_3}^{\alpha_4} \sin \alpha \left( \left( \frac{ad}{2} \right)^2 + (r \cos \alpha)^2 + (y - r \sin \alpha)^2 \right)^{-\frac{3}{2}} d\alpha \right) \quad (8)$$

where  $a$ ,  $l$ ,  $d$ ,  $h$ ,  $r$ ,  $\alpha_1$ ,  $\alpha_2$ ,  $\alpha_3$ , and  $\alpha_4$  are  $l/d$ , the length of the straight coil, the distance between the straight coils located along the  $z$ -axis, the distance between the straight coils located along the  $y$ -axis, the radius of the arc coil, and the starting and ending angles of the upper and lower arc coils, respectively. The signs of  $\mp$  in (7) and  $\pm$  in (8) correspond to the cases of the gradient saddle coil and the uniform saddle coil where the current in the upper and the lower part of the saddle coil flows in the opposite and the same direction, respectively. To obtain the geometrical relationship of the gradient saddle coil, the magnetic fields in the  $y$ -direction from the straight and arc coils should satisfy the following conditions:

$$\left. \frac{dH_y^{st,arc}}{dy} \right|_{y=0} = \text{const.}, \quad \left. \frac{d^2 H_y^{st,arc}}{dy^2} \right|_{y=0} = 0 \\ \left. \frac{d^3 H_y^{st,arc}}{dy^3} \right|_{y=0} = 0. \quad (9)$$

The third condition of (9) provides the relationship between  $a$  and  $h$ . Fig. 3 shows the geometrical relationship of the gradient saddle coil and the magnetic field distribution in the  $xy$ -plane. The linearized magnetic field of the gradient saddle coil near the center can be expressed as follows:

$$\vec{H}_g = [g_g x - 2.4398g_g y \ 1.4398g_g z]^T \quad (10)$$

$$g_g = \cos^{-1} \left( 1 - \frac{3}{2a^2} \right) \frac{16}{3\pi} \left( \frac{3}{7} \right)^{\frac{5}{2}} \frac{i_g}{r_g^2} \text{ for } a \cong 1.2015 \quad (11)$$

where  $i_g$  and  $r_g$  are the current and radius of the gradient saddle coil, respectively.

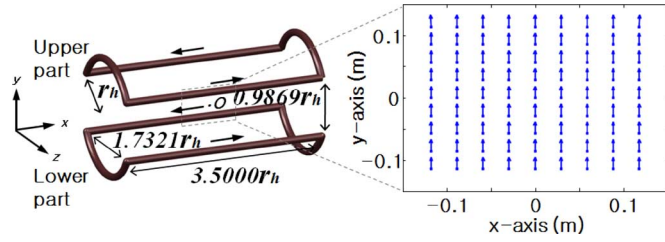


Fig. 4. Geometrical relationship and magnetic field of the uniform saddle coil.

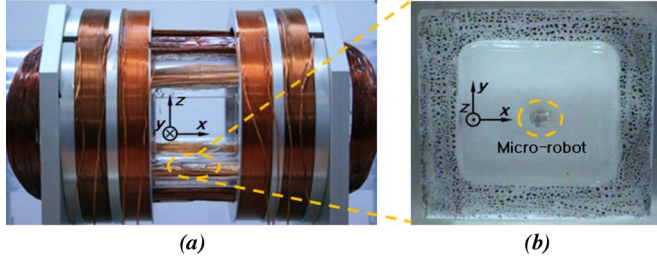


Fig. 5. Experimental setup of (a) proposed MNS and (b) micro-robot in silicone oil.

The uniform saddle coil, in which the currents in the upper and lower coils flow in the same direction should satisfy the following conditions:

$$\left. \frac{dH_y^{st,arc}}{dy} \right|_{y=0} = 0, \quad \left. \frac{d^2 H_y^{st,arc}}{dy^2} \right|_{y=0} = 0. \quad (12)$$

The second condition of (12) provides the relationship between  $a$  and  $h$ . Fig. 4 shows the geometrical relationship of the uniform saddle coil and the magnetic field distribution in the  $xy$ -plane. The linearized magnetic field of the gradient saddle coil near the center can be expressed as follows:

$$\vec{H}_u = [0 \ d_u \ 0]^T \quad (13)$$

$$d_u = 0.6004 \frac{i_u}{r_u} \quad (14)$$

where  $i_u$  and  $r_u$  are the current and radius of the uniform saddle coil, respectively.

### C. Development of a Novel MNS

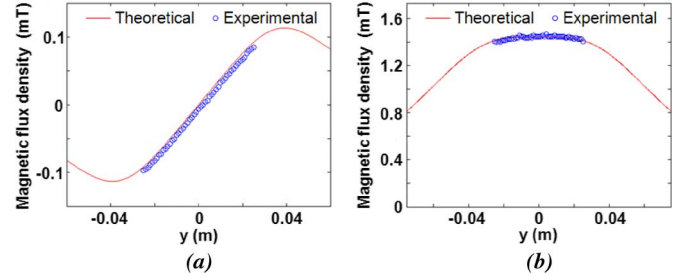
This research utilizes one pair of Maxwell and Helmholtz coils and one pair of gradient and uniform saddle coils to develop the proposed MNS as shown in Fig. 1. The magnetic field near the center of the MNS can be expressed as follows:

$$\vec{H}_{MNS} = [d_h + (g_g + g_m)x \ d_u + (-2.4398g_g - 0.5g_m)y \ (1.4398g_g - 0.5g_m)z]^T. \quad (15)$$

Since the uniform magnetic field exists only in the  $xy$ -plane, the micro-robot can be aligned within the  $xy$ -plane. Assuming that the micro-robot is initially positioned along the line with an angle of  $\phi$  from the  $x$ -axis, the micro-robot is to be aligned to an angle of  $\theta$ . With (6) and (14), the condition of a uniform

TABLE I  
MAJOR SPECIFICATIONS OF THE PROPOSED NOVEL MNS

Coil	Radius (mm)	Diameter of copper wire (mm)	Coil turns
Maxwell coil	78.0	1.1	180
Helmholtz coil	80.0	1.0	144
Gradient saddle coil	50.0	0.8	101
Uniform saddle coil	62.5	0.7	120

Fig. 6. Magnetic flux density distribution along the  $y$ -axis for (a) gradient saddle coil with  $i_g = 1$  A and (b) uniform saddle coil with  $i_u = 1$  A.

magnetic field along the  $\theta$  direction produces the following relationships of the currents between the uniform saddle coil and Helmholtz coil, and the magnetic torque:

$$i_u = 1.1917 \tan \theta \frac{r_u}{r_h} i_h \quad (16)$$

$$\vec{T} = 0.7155 \mu_0 M V \sec \theta \sin(\theta - \phi) \frac{i_h}{r_h} \hat{k}. \quad (17)$$

Once the torque aligns the micro-robot along the  $\theta$  direction, the micro-robot can be propelled by the magnetic force which is generated along that direction. The magnetic force from the Maxwell and gradient saddle coils should satisfy the following condition in order to propel the micro-robot along the aligned angle of  $\theta$ :

$$\frac{F_y}{F_x} = \frac{\mu_0 M V \sin \theta (-2.4398g_g - 0.5g_m)}{\mu_0 M V \cos \theta (g_g + g_m)} = \frac{\sin \theta}{\cos \theta}. \quad (18)$$

Equation (18) determines the relationship of the currents applied to the Maxwell and gradient saddle coils. By applying (1), the magnetic force is determined as follows:

$$i_m = -1.1751 \left( \frac{r_m}{r_g} \right)^2 i_g \quad (19)$$

$$\vec{F} = 0.3616 \mu_0 M V \frac{i_m}{r_m^2} (\cos \theta \hat{i} + \sin \theta \hat{j}). \quad (20)$$

Equation (20) states that the magnetic force of a micro-robot is always in the direction of the magnetization with a constant magnitude regardless of its direction once the relationship in (19) is satisfied. Therefore, the aligning and propelling motion of a micro-robot can be realized in the proposed MNS by controlling the currents of the coils.

### III. RESULTS AND DISCUSSION

The proposed MNS was constructed as shown in Fig. 5. Table I shows the major specifications of the proposed MNS.



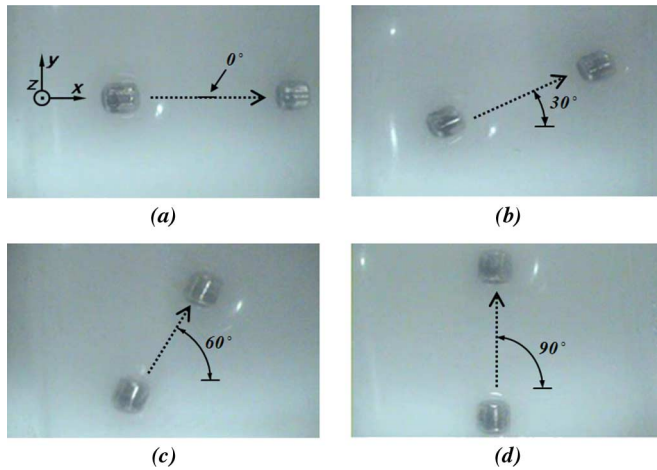


Fig. 7. Aligning and propelling motion of a micro robot with (a)  $\theta = 0^\circ$ , (b)  $\theta = 30^\circ$ , (c)  $\theta = 60^\circ$ , and (d)  $\theta = 90^\circ$ .

TABLE II

MAGNETIC FORCES OF THE CONVENTIONAL AND PROPOSED MNS ALONG AN ANGLE OF  $30^\circ$  (MC: MAXWELL COIL, GSC: GRADIENT SADDLE COIL)

MNS	Coil	Radius (mm)	Current (A)	$ \vec{F} $ ( $\mu\text{N}$ )
Conventional	MC 1	100	100	24.18
	MC 2	200	400	
Proposed	MC	100	100	27.27
	GSC	100	85.1	

TABLE III

MAGNETIC TORQUES OF THE CONVENTIONAL AND PROPOSED MNS ALONG AN ANGLE OF  $30^\circ$  (HC: HELMHOLTZ COIL, USC: UNIFORM SADDLE COIL)

MNS	Coil	Radius (mm)	Current (A)	$ \vec{T} $ ( $\mu\text{N} \cdot \text{m}$ )
Conventional	HC 1	100	100	3.11
	HC 2	200	115.5	
Proposed	HC	100	100	3.11
	USC	100	68.8	

The magnetic field generated by the gradient saddle coil and the uniform saddle coil is measured by using a Gauss-meter. Fig. 6 shows that the measured magnetic flux densities along the  $y$ -axis near the center of the coils match well with the theoretically calculated ones. The micro-robot is a cylindrical neodymium magnet whose diameter, length, and magnetization are 2 mm, 2 mm, and 955 000 A/m along the axial direction, respectively. The micro-robot was placed in the center of a dish filled with silicone oil, which has a high viscosity of 350 cP. Silicon oil reduces the abrupt motion of the micro-robot. The aligning and propelling motions of the micro-robot are achieved by controlling the currents of the proposed MNS. Fig. 7 shows overlapped pictures from an experiment in which a micro-robot

was aligned and propelled along the angles of  $0^\circ$ ,  $30^\circ$ ,  $60^\circ$ , and  $90^\circ$ . It shows that the proposed MNS successfully aligns and propels a micro-robot in a plane.

The performance of the proposed MNS was compared with the conventional two pairs of Maxwell and Helmholtz coils in [6]. In the conventional MNS, the radius of the Helmholtz coil in the  $x$ -axis should theoretically be at least two times larger than the radius of the Helmholtz coil in the  $y$ -axis because of the geometrical constraint of the Helmholtz coil. This geometrical restriction in the conventional MNS makes the construction ineffectively large. On the other hand, the proposed MNS theoretically uses the same radius for the Maxwell coil, Helmholtz coil, gradient saddle coil, and uniform saddle coil so that the overall structure is compact and suitable for a patient to lie down along the MNS as shown in Fig. 1.

The magnetic torque to align the micro-robot from  $0^\circ$  to  $30^\circ$  and the magnetic force to propel it along  $30^\circ$  were theoretically examined, considering the same effective region in the conventional and the proposed MNS. Table II shows that the proposed MNS generates a 12.8% larger magnetic force than the conventional one even though the applied current to the gradient saddle coil is 78.7% smaller than that applied to the Maxwell coil of the conventional MNS. And Table III shows that the applied current to the uniform saddle coil is 30.4% smaller than the current applied to the Helmholtz coil of the conventional MNS to produce the same magnetic torque.

#### IV. CONCLUSION

This research developed a novel MNS that is more geometrically compact and magnetically efficient than conventional MNS. It can contribute to the effective manipulation of micro-robots in human blood vessels.

#### ACKNOWLEDGMENT

This work was supported by the Strategy Technology Development Program (No. 10030037) of the Korean Ministry of Knowledge Economy.

#### REFERENCES

- [1] American Heart Association & American Stroke Association, Dallas, TX, "Heart disease and stroke statistics," 2007.
- [2] S. Saito, S. Tanaka, Y. Hiroe, Y. Miyashita, S. Takahashi, S. Satake, and K. Tanaka, "Angioplasty for chronic total occlusion by using tapered-tip guidewires," *Catheterization Cardiovascular Interventions*, vol. 3, no. 59, pp. 305–311, 2003.
- [3] K. Ishiyama, K. I. Arai, M. Sendoh, and A. Yamazaki, "Spiral-type micro-machine for medical applications," *J. Micromechatronics*, vol. 2, no. 1, pp. 77–86, 2003.
- [4] S. Tamaz, R. Gourdeau, A. Chanu, J. B. Mathieu, and S. Martel, "Real-time MRI-based control of a ferromagnetic core for endovascular navigation," *IEEE Trans. Biomed.*, vol. 55, no. 7, pp. 1854–1863, Jul. 2008.
- [5] K. B. Yesin, K. Vollmers, and B. J. Nelson, "Modeling and control of untethered biomicrobots in a fluidic environment using electromagnetic fields," *Int. J. Robot. Res.*, vol. 25, pp. 527–536, 2006.
- [6] H. Choi, J. Choi, G. Jang, J. Park, and S. Park, "Two dimensional actuation of micro-robot with stationary two-pair coils system," *Smart Mater. Structures*, vol. 18, pp. 1–9, 2009.